Arthritis & Rheumatology
Vol. 73, No. 11, November 2021, pp 2127–2137
DOI 10.1002/art.41781

American College of Rheumatology
Empowering Rheumatology Professionals

Prediction of Differential Pharmacologic Response in Chronic Pain Using Functional Neuroimaging Biomarkers and a Support Vector Machine Algorithm: An Exploratory Study

Eric Ichesco,[1] Scott J. Peltier,[1] Ishtiaq Mawla,[1] Daniel E. Harper,[1] Lynne Pauer,[2] Steven E. Harte,[1] Daniel J. Clauw,[1] and Richard E. Harris[1]

Objective. There is increasing demand for prediction of chronic pain treatment outcomes using machine-learning models, in order to improve suboptimal pain management. In this exploratory study, we used baseline brain functional connectivity patterns from chronic pain patients with fibromyalgia (FM) to predict whether a patient would respond differentially to either milnacipran or pregabalin, 2 drugs approved by the US Food and Drug Administration for the treatment of FM.

Methods. FM patients participated in 2 separate double-blind, placebo-controlled crossover studies, one evaluating milnacipran (n = 15) and one evaluating pregabalin (n = 13). Functional magnetic resonance imaging during rest was performed before treatment to measure intrinsic functional brain connectivity in several brain regions involved in pain processing. A support vector machine algorithm was used to classify FM patients as responders, defined as those with a ≥20% improvement in clinical pain, to either milnacipran or pregabalin.

Results. Connectivity patterns involving the posterior cingulate cortex (PCC) and dorsolateral prefrontal cortex (DLPFC) individually classified pregabalin responders versus milnacipran responders with 77% accuracy. Performance of this classification improved when both PCC and DLPFC connectivity patterns were combined, resulting in a 92% classification accuracy. These results were not related to confounding factors, including head motion, scanner sequence, or hardware status. Connectivity patterns failed to differentiate drug nonresponders across the 2 studies.

Conclusion. Our findings indicate that brain functional connectivity patterns used in a machine-learning framework differentially predict clinical response to pregabalin and milnacipran in patients with chronic pain. These findings highlight the promise of machine learning in pain prognosis and treatment prediction.

INTRODUCTION

Suboptimal management of chronic pain has contributed to a pain-related health crisis, including the ongoing opioid epidemic in the US. As a result, discovery of biologic markers of pain to supplement self-report measures of clinical pain has been garnering attention, and become a priority for organizations like the National Institutes of Health (e.g., The Helping to

ClinicalTrials.gov identifiers: NCT00760474 and NCT01173055.
Supported by Pfizer (grant A0081211) and Forest Laboratories (grant MD-SAV-09).
[1]Eric Ichesco, BS, Scott J. Peltier, PhD, Ishtiaq Mawla, MS, Daniel E. Harper, PhD, Steven E. Harte, PhD, Daniel J. Clauw, MD, Richard E. Harris, PhD: University of Michigan, Ann Arbor; [2]Lynne Pauer, MS: Pfizer Inc., Groton, Connecticut.
Mr. Ichesco and Dr. Peltier contributed equally to this work.
Ms Pauer owns stock or stock options in Pfizer. Dr. Harte has received consulting fees from Forest Laboratories, Aptinyx, and Arbor Medical Innovations (less than $10,000 each) and research support from Forest Laboratories. Dr. Clauw has received consulting fees, speaking fees, and/or honoraria from Pfizer, Abbott, Aptinyx, Cerephex, Daiichi Sankyo, Eli Lilly, Lundbeck Pharmaceuticals, Pierre Fabre Laboratories, Theravance, Williams & Connolly, LLP, Zynerba, Astella, and Forest Laboratories (less than $10,000 each) and from Samumed, Tonix, and Nix Patterson, LLP (more than $10,000 each) and research support from Aptinyx, Cerephex, Pfizer, and Forest Laboratories. Dr. Harris has received consulting fees from Pfizer and Aptinyx (less than $10,000 each) and research support from Pfizer. No other disclosures relevant to this article were reported.
Upon request, and subject to review, Pfizer will provide the data that support the findings of this study. Subject to certain criteria, conditions and exceptions, Pfizer may also provide access to the related individual anonymized participant data. See https://www.pfizer.com/science/clinical-trials/trial-data-and-results for more information.
Address correspondence to Eric Ichesco, BS, Chronic Pain and Fatigue Research Center, Department of Anesthesiology, University of Michigan, Ann Arbor, MI. Email: eichesco@med.umich.edu.
Submitted for publication June 16, 2020; accepted in revised form April 20, 2021.

End Addiction Long-term [HEAL] initiative [heal.nih.gov]). Ultimately, such biomarkers will aid diagnosis, forecast longitudinal outcomes, and predict treatment efficacy.

One clinical pain disorder where biomarker development has become imperative is fibromyalgia (FM), a chronic condition characterized by widespread pain, fatigue, hypersensitivity to sensory stimuli (1), and increased prevalence of multiple negative health outcomes. Research in the past 2 decades has shown that augmented pain and sensory processing in the central nervous system is a primary mechanism underlying pain in FM patients (2,3). Multiple brain loci have been identified as being related to FM pain, including subregions of the salience, default mode, and somatosensory networks (3,4). Some regions of the default mode network have been shown to have increased connectivity to the salience and somatosensory networks in FM. This type of connectivity might be a marker for chronic pain intensity in this population (3,4).

Functional magnetic resonance imaging (fMRI) studies have demonstrated that aberrant pain processing in FM can be modulated with US Food and Drug Administration–approved pharmacologic compounds, such as pregabalin, milnacipran, and duloxetine. However, only 30% of FM patients report clinically significant pain improvements with any of these drugs (5–7). Patients who fail to receive immediate analgesic effects may receive other treatments in a "trial and error" approach that is both inefficient and costly. The identification of tools that can predict the effectiveness of specific pharmacologic agents used to treat pain at the individual patient level would be of significant clinical benefit and an important step toward personalized analgesia.

With the advent of sophisticated multivariate data analytic techniques such as machine learning, prediction of analgesic response from neuroimaging data has become a promising avenue for biomarker development (8). Briefly, machine-learning techniques "learn" the underlying data patterns (e.g., neuroimaging voxels) to form a model using labels (e.g., pregabalin responder versus milnacipran responder), which can then be applied to unseen or new data to make predictions. Such models have rarely been used in clinical pain populations to predict treatment efficacy. To the best of our knowledge, this study is the first to assess fMRI-derived biomarkers as predictors of differential analgesic response in chronic pain.

We built machine-learning models, using a support vector machine (SVM), from fMRI data obtained from 2 separate, double-blind, placebo-controlled crossover trials in FM patients, one with pregabalin (9) and another with milnacipran (10). These 2 medications are thought to work differently on pain processing, with pregabalin reducing pain-promoting neural activity (9) and milnacipran increasing pain inhibitory pathways (10). We reasoned that given the central mechanisms of action of the 2 drugs, pretreatment brain connectivity (i.e., communication between brain structures) might be able to differentially predict drug responsiveness.

PATIENTS AND METHODS

Subjects. Fifty women with FM who were previously enrolled in 2 independent double-blind, placebo-controlled crossover studies investigating the effects of pregabalin versus placebo and milnacipran versus placebo (9,10) were eligible for this secondary analysis (Consolidated Standards of Reporting Trials [CONSORT] diagrams are included in Supplementary Figures 1 and 2, available on the *Arthritis & Rheumatology* website at http://onlinelibrary.wiley.com/doi/10.1002/art.41781/abstract). Twenty-seven FM patients were enrolled in the original pregabalin study. A total of 14 patients were excluded (9 were excluded in the original study) (9). Five additional patients were excluded from the present study: 4 for head motion using more stringent translational or rotational thresholds after assessment of brain images (see below for additional details), and 1 for incomplete clinical data. This resulted in 13 patients taking pregabalin being included in the present analysis. Twenty-three female patients with FM were enrolled in the original milnacipran study (8 were excluded as previously reported) (10). Brain images for the remaining 15 patients passed quality inspection and were included in the present analysis.

All study participants gave written informed consent. Study protocols and informed consent documents were approved by the University of Michigan Institutional Review Board and the sponsor of the respective studies: Pfizer for pregabalin and Forest Laboratories for milnacipran. All clinical symptom data from both trials were previously verified for accuracy and the database was locked before analysis. Neuroimaging data were stored, validated, analyzed, and assessed for quality at the University of Michigan independent of Pfizer and Forest Laboratories personnel. Patient demographic characteristics, medications, inclusion/exclusion criteria, and treatment effects have been reported previously (9,10). Patient demographic characteristics and medications are listed in Table 1, while brief descriptions of the inclusion and exclusion criteria are included in the Supplementary Methods, available on the *Arthritis & Rheumatology* website at http://onlinelibrary.wiley.com/doi/10.1002/art.41781/abstract.

Clinical pain and mood measures. For participants enrolled in the pregabalin study, clinical pain was assessed using a 10-cm visual analog scale (VAS) bounded by the anchors "no pain" and "worst pain imaginable." Subjects from the milnacipran study reported their clinical pain with an itemized question from the Brief Pain Inventory (BPI) that ranged from 0–10, where 0 was anchored with the words "no pain" and 10 was anchored with the words "pain as bad as you can imagine" (11). Depression and anxiety were assessed using the Hospital Anxiety and Depression Scale (HADS), a 14-item measure with each item rated on a 4-point severity scale (12). The HADS produces 2 scales, one for anxiety and one for depression. The BPI, VAS, and HADS were administered prior to the baseline neuroimaging session. Differences in clinical pain and mood were measured using

Table 1. Characteristics of the patients with FM, and medications taken, in the pregabalin and milnacipran studies*

Patient	Age, years	Race	BMI	Medications and supplements
Pregabalin study				
1	44	White	25	Augmentin, Motrin
2	29	White	21	Albuterol, erythromycin eye lotion, Extra Strength Tylenol, ibuprofen, Ortho Tri-Cyclen, Zantac, Zyrtec
3	25	White	23	Children's Tylenol Plus Cough and Runny Nose, Motrin
4	43	White	25	Triamcinolone acetonide 0.5%
5	36	White	21	Amoxicillin, Augmentin, Motrin, Synthroid, Tylenol
6	42	White	27	Sudafed, Tylenol, Zyrtec
7	42	White	26	Advil, CVS Sinus Allergy, Effexor, Nyquil, Tylenol
8	39	White	25	Claritin, melatonin, NuvaRing, propionate fluticasone, Tylenol
9	44	White	30	Amoxicillin, Nyquil, prednisone, Proventil, Rocephin, Tylenol
10	59	White	29	Colchicine, Flexeril, hydrochlorothiazide, melatonin, nabumetone, Omacor, Prilosec trazodone
11	19	White	23	Bupropion, Concerta, Loestrin
12	19	White	26	Claritin, Concerta, Loestrin
13	39	White	25	Effexor, Excedrin ES, fluticasone propionate nasal spray, ibuprofen, Maxalt, Proventil HFA, pseudoephedrine, Seasonale, Topamax, zonisamide
Milnacipran study				
1	54	White	33	Tramadol
2	26	White	36	Pregabalin, metformin
3	30	White	31	Metronidazole, Benadryl, Motrin
4	42	White	27	Ibuprofen, Sudafed
5	53	White	33	Dinox, Anacin, Aleve, ibuprofen, prednisone, Mobic, Mucinex, Ventolin, Airborne
6	36	African American	37	Amlodipine besylate, lisinopril/hydrochlorothiazide, Aleve
7	40	White	24	NuvaRing, ibuprofen, Skelaxin, Vicodin, Tylenol, Quasense
8	36	White	21	Synthroid, Tylenol, acetaminophen, Motrin, ibuprofen
9	39	White	21	Nasonex
10	50	White	29	Lisinopril/hydrochlorothiazide, amoxicillin
11	30	White	28	Xanax, Cataphlam, Aleve
12	40	White	23	Motrin
13	53	African American	26	Motrin, Excedrin
14	27	White	32	Levothyroxine, Singulair, albuterol sulfate, Vicodin, cyclobenzaprine, Maxalt, Tylenol, Cortizone shots, cephalexin
15	55	White	35	Avapro, Norvasc, Aldactazide, Detrol LA, pregabalin, Synthroid, Taclonex, Diprolene Gel, aspirin, Tylenol, Motrin, minocycline, methotrexate

* FM = fibromyalgia; BMI = body mass index.

paired-sample *t*-tests (predrug versus postdrug). In both studies, drug responders were defined as those who had a reduction in clinical pain of ≥20% from predrug to postdrug, since this criterion provided a sufficient number of subjects who did respond to either drug for meaningful SVM classification (see below). In both studies, anxiety/depression responders were defined as those who had a decrease in anxiety or depression, and nonresponders were defined as having no change or an increase in anxiety or depression.

Resting-state functional connectivity MRI as predictive of drug response. *Data acquisition.* Functional connectivity MRIs, including a 6-minute resting-state scan and a high-resolution T1 structural scan, were acquired for all participants at baseline. All scans were performed on a 3.0T GE Signa Scanner (LX VH3 release, quadrature birdcage transmit–receive radiofrequency coil, neuro-optimized gradients). Resting-state fMRI data for both studies were acquired using a custom T2*-weighted spiral-in sequence (repetition time [TR] 2,000 msec, echo time [TE] 30 msec, flip angle 90°, matrix size 64 × 64 pixels with 43 slices, and 3.13 × 3.13 × 3 mm voxels; 5 discarded dummy acquisitions). During each resting-state scan (180 volumes), participants were asked to remain awake with eyes open. To reduce head motion, participants' heads were secured in the head coil using foam padding around the sides of the head and a strap across the forehead. A fixation cross was displayed on a presentation screen. Participants were asked to lie still and fixate on the cross throughout the scan. It has been shown that cognitive tasks such as staring at a cross do not typically disrupt resting-state networks (13).

Physiologic data were collected simultaneously with fMRI data because cardiorespiratory fluctuations are known to influence fMRI intrinsic connectivity within several brain networks. Cardiac data were collected for each participant using an infrared pulse oximeter (GE) attached to the right middle finger. Respiratory volume data were acquired using a GE magnetic resonance–compatible chest plethysmograph that was secured around the abdomen. Further, previously mentioned T1 high-resolution images were acquired using a spoiled gradient-echo inversion recovery sequence (for the pregabalin study: TR 10.5 msec, TE 3.4 msec, flip angle 25°, matrix size 256 × 256 pixels with 106 slices, and 0.94 × 0.94 × 1.5 mm voxels; for the milnacipran study: TR 1,400 msec, TE 1.8 msec, flip angle 15°, matrix size 256 × 256 pixels with 124 slices, and 1.02 × 1.02 × 1.2 mm voxels). Inspection of individual T1 MRIs revealed no gross morphologic abnormalities for any participant.

Preprocessing. Data were preprocessed and analyzed using FSL (www.fmrib.ox.ac.uk/fsl) and statistical parametric mapping (SPM) (version 8; Functional Imaging Laboratories) as well as the functional connectivity toolbox Conn (Cognitive and Affective Neuroscience Library, Massachusetts Institute of Technology) (14) and the GIFT toolbar (15). Following collection of functional data, cardiorespiratory artifacts were corrected for using RETROICOR (16). Subsequent preprocessing steps were conducted within SPM and included motion correction (realignment to the first image of the time series), registration of all images to the mean motion-corrected functional image, normalization to the standard SPM Montreal Neurological Institute template (generating 2 × 2 × 2 mm resolution images), and spatial smoothing (convolution with an 8-mm full-width half-maximum Gaussian kernel). Head motion from each participant was assessed by evaluating 3 translations and 3 rotations. Translational thresholds were set to ±2 mm. Rotation thresholds were limited to ±1°. Subjects were excluded from the analysis if head motion exceeded either of the thresholds in 1 of the 6 dimensions.

Seed-to–whole brain functional connectivity maps were generated using the Conn toolbox (14). Within the Conn toolbox, seed regions' time series were extracted; white matter, cerebrospinal fluid, and realignment parameters were entered into the analysis as covariates of no interest. A band-pass filter (frequency window 0.01–0.1 Hz) was applied, thus removing linear drift artifacts and high-frequency noise. First-level analyses were performed correlating seed region time series signal with averaged time series voxel signal throughout the whole brain, thereby creating bivariate Fisher Z-transformation correlation seed region–to-voxel connectivity maps (one map per seed per individual). Machine-learning analyses were implemented using a linear SVM, performed using the libsvm toolbox version 3.18 (17) in MATLAB 7.5b.

Our prior studies (9,10) identified regions with functional connectivity patterns that were related to drug response to pregabalin and milnacipran. We therefore chose these as seed regions to test responders to the 2 drugs in a machine-learning framework for prediction. These seed regions encompass various known ascending and descending pain circuits in the brain. Seed-to–whole brain functional connectivity maps were generated for the following regions (Supplementary Table 1, available on the *Arthritis & Rheumatology* website at http://onlinelibrary.wiley.com/doi/10.1002/art.41781/abstract): the left posterior cingulate cortex (PCC) and left inferior parietal lobule (based on pregabalin study results) (9) and the bilateral periaqueductal gray, subgenual anterior cingulate cortex (ACC), perigenual ACC, dorsal ACC, and bilateral dorsolateral prefrontal cortex (DLPFC) (based on milnacipran study results) (10).

Support vector machine classification. Machine-learning analyses were implemented using a linear SVM, performed using the libsvm toolbox version 3.18 (https://www.csie.ntu.edu.tw/~cjlin/libsvm/) in MATLAB 7.5b. Briefly, linear SVM tries to separate 2 distinct classes (i.e., pregabalin responder versus milnacipran responder) of features (i.e., data from brain voxels) by creating a hyperplane that separates the 2 classes in the most optimal manner. SVM was implemented on brain connectivity maps of pregabalin responders versus milnacipran responders. SVM classification was performed using a linear kernel with parameter C = 1 (no improvement was found using a C parameter line search), and while it is true that a nonlinear kernel may capture higher-order features, we found no advantage to using a radial basis function with this data set.

Leave-one-out cross-validation was used to calculate classification accuracies and predicted values. Accuracies >75% for identifying a drug responder were deemed clinically significant. SVM model weights were averaged across all leave-one-out iterations to investigate the spatial distribution of the classification weights. Significance levels for the model weights were generated by permuting the treatment labels 100 times for each leave-one-out instance, resulting in 1,300 model weight instances for each voxel location for the pregabalin responder versus milnacipran responder analysis, allowing significance to be calculated by the number of times a model weight occurred in the histogram. Significant values ($P < 0.05$) were overlaid on reference anatomy, and the connectivity maps of the most significant areas were plotted to examine their relationship to the multivariate pattern. A chance-level classification outcome was taken to reaffirm that the given predictive model was specific and minimally affected by confounders.

To determine if predrug VAS ratings can predict responders to pregabalin versus responders to milnacipran with high accuracy, we performed a logistic regression analysis. Then, to investigate if there was an additive effect on classification accuracy, we included predrug clinical pain ratings as a vector to the connectivity maps of each patient and performed SVM classification.

Assessment of confounders and investigation of separation accuracy in SVM classification. Subsequent steps were taken to confirm that a classifier did not possess any confounders. First, to confirm the specificity of the pregabalin versus milnacipran

classifier to responders, the model was also tested in the nonresponders. Second, since milnacipran is an antidepressant, we also investigated whether the classifier was specific to predicting changes in pain as opposed to changes in anxiety or depression using the HADS questionnaire (12). The model was first tested in pregabalin responders versus milnacipran responders for depression, and was then tested in responders versus nonresponders with regard to anxiety and depression (where a responder was defined as having a decrease in anxiety or depression and a nonresponder was defined as having no change or an increase in anxiety or depression). Third, to investigate whether subject motion influenced the classification, the model was tested in high-motion versus low-motion groups. Finally, to confirm that the classifier was not predicting differences in sequence and hardware status between the pregabalin and milnacipran studies, an SVM analysis was performed comparing baseline placebo scans for all seeds between the 2 studies. This SVM analysis was performed exactly as was described above for the responder versus responder analysis, except that the input was placebo data for all subjects from both studies (n = 13 for pregabalin and n = 15 for milnacipran).

RESULTS

Subject demographic characteristics, clinical pain, and psychological measures. There was no significant difference in age between patients in the 2 studies (mean ± SD 35.7 ± 11.4 years in the pregabalin study and 40.7 ± 10.2 in the milnacipran study; P = 0.228). Pregabalin responders (n = 6) and milnacipran responders (n = 7) reported less pain after

Table 2. Clinical pain, anxiety, and depression in all FM patients and responders/nonresponders to pregabalin or milnacipran based on pain improvement*

	Pretreatment	Posttreatment	*P*
Clinical pain, 0–10-cm VAS			
Pregabalin study			
Responders	5.4 ± 2.5	1.6 ± 2.3	0.0003
Nonresponders	1.3 ± 1.0	1.7 ± 2.3	0.60
All patients	3.2 ± 2.7	1.7 ± 1.9	0.06
Milnacipran study			
Responders	5.6 ± 1.5	2.1 ± 2.0	0.00009
Nonresponders	4.8 ± 2.4	6.0 ± 2.6	0.13
All patients	5.1 ± 2.0	4.2 ± 3.0	0.23
Pretreatment clinical pain, 0–10-cm VAS			0.85
Pregabalin responders	5.4 ± 2.5	–	
Milnacipran responders	5.6 ± 1.5	–	
Anxiety and depression data			
Pregabalin study			
HADS anxiety score			
Responders	9.5 ± 2.3	7.8 ± 4.9	0.31
Nonresponders	2.9 ± 2.9	2.6 ± 3.2	0.17
All patients	5.9 ± 4.3	5.0 ± 4.7	0.40
HADS depression score			
Responders	6.5 ± 3.3	4.0 ± 3.8	0.22
Nonresponders	1.7 ± 2.2	2.3 ± 2.4	0.46
All patients	3.9 ± 3.6	3.1 ± 3.1	0.40
Milnacipran study			
HADS anxiety score			
Responders	7.0 ± 3.5	3.9 ± 3.1	0.01
Nonresponders	6.1 ± 2.5	5.6 ± 3.3	0.53
All patients	6.5 ± 2.9	4.8 ± 3.3	0.02
HADS depression score			
Responders	4.9 ± 3.0	3.1 ± 2.9	0.03
Nonresponders	4.1 ± 2.5	4.5 ± 2.1	0.53
All patients	4.5 ± 2.7	3.9 ± 2.5	0.24
Pretreatment HADS anxiety score			0.16
Pregabalin responders	9.5 ± 2.3	–	
Milnacipran responders	7.0 ± 3.5	–	
Pretreatment HADS depression score			0.37
Pregabalin responders	6.5 ± 3.3	–	
Milnacipran responders	4.9 ± 3.0	–	

* Responders were defined as having a ≥20% reduction in clinical pain (on a visual analog scale [VAS]) following treatment. The pregabalin sample included 13 patients (46% were responders [n = 6]; 54% were nonresponders [n = 7]). The milnacipran sample included 15 patients (47% were responders [n = 7]; 53% were nonresponders [n = 8]). Values are the mean ± SD. FM = fibromyalgia; HADS = Hospital Anxiety and Depression Scale.

receiving the drug compared to nonresponders. Full results for clinical pain effects in responders, nonresponders, and all patients are shown in Table 2. Results for anxiety and depression in these groups (responders and nonresponders determined by clinical pain improvement) are included in Table 2. We focused our analyses on the ability of pretreatment functional connectivity MRI to predict differential analgesic responsiveness.

Differential classification of response to pregabalin versus milnacipran. We were unable to predict differential response to pregabalin versus milnacipran using predrug clinical pain ratings (62% accuracy; $\beta = -0.065$, $P = 0.782$). Whole-brain connectivity patterns to the left PCC seed differentiated pregabalin responders from milnacipran responders with 77% accuracy (Figure 1A). Significant average model weights

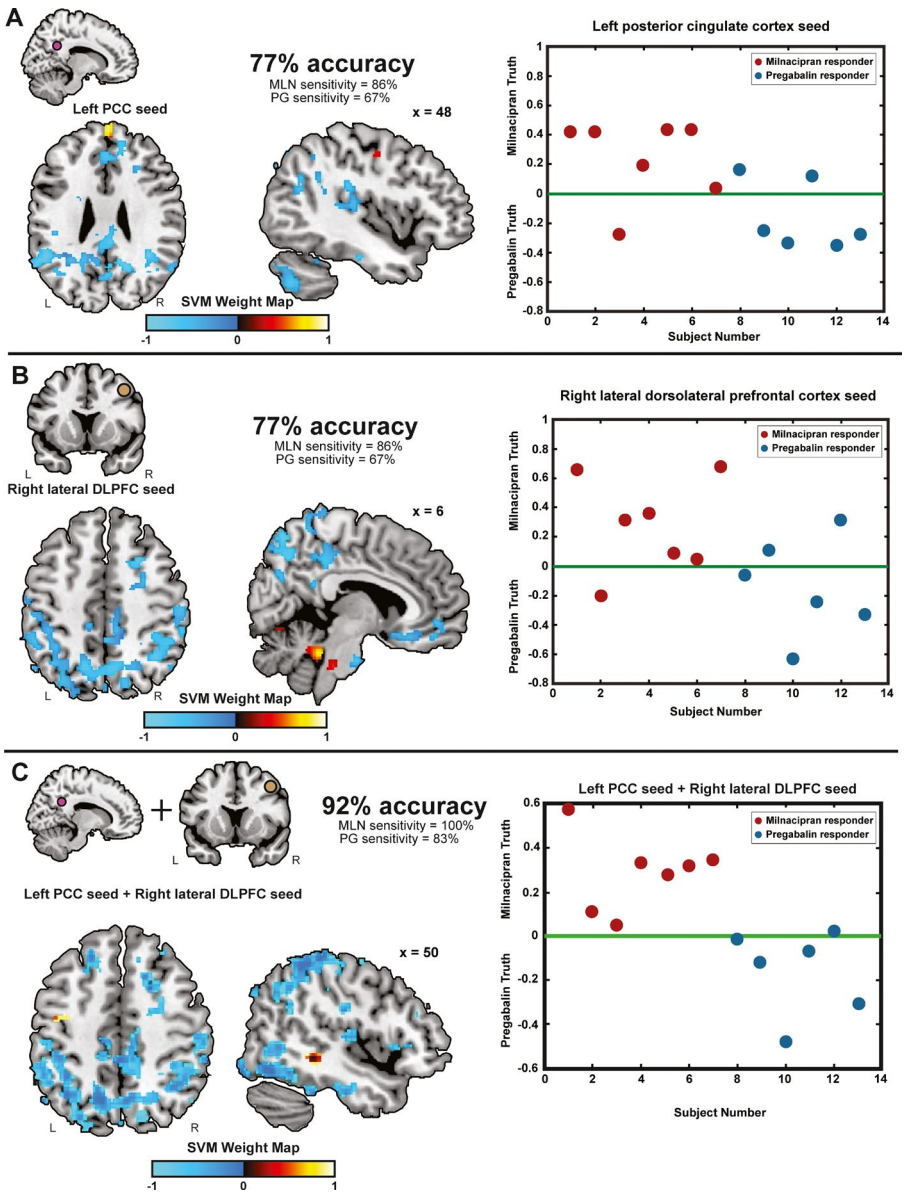

Figure 1. Baseline resting-state functional connectivity between the seed region (posterior cingulate cortex [PCC] or right lateral dorsolateral prefrontal cortex [DLPFC]) and whole brain differentiates patients with fibromyalgia (FM) who respond to pregabalin (PG) from patients with FM who respond to milnacipran (MLN) with high accuracy. **A**, Resting-state functional connectivity between the left PCC seed and regions including the precuneus, inferior parietal lobule, PCC, and left insular cortex classifies pregabalin responders versus milnacipran responders with 77% accuracy. **B**, Resting-state functional connectivity between the right lateral DLPFC seed and regions including the superior parietal lobule, precuneus, primary somatosensory cortex, and left insular cortex classifies pregabalin responders versus milnacipran responders with 77% accuracy. **C**, Baseline resting-state functional connectivity between the left PCC and the right lateral DLPFC seeds combined and the superior parietal lobule, precuneus, perigenual anterior cingulate cortex, mid cingulate cortex, and PCC classifies pregabalin responders versus milnacipran responders with 92% accuracy. Warm colors (red to yellow) designate positive support vector machine (SVM) weights where milnacipran responders have greater connectivity compared to pregabalin responders; cool colors (dark blue to light blue) designate negative SVM weights where pregabalin responders have more connectivity compared to milnacipran responders. Graphs show prediction values for each subject.

contributing to successful classification included greater connectivity for pregabalin responders versus milnacipran responders to regions such as the left inferior parietal lobule, left precuneus, left and right PCC, right perigenual ACC, and right primary motor/somatosensory cortex. In addition, significant average model weights where connectivity to the left PCC was found to be greater for milnacipran responders as compared to pregabalin responders included the left primary visual cortex, bilateral superior medial frontal gyrus, bilateral superior parietal lobule, and the right superior temporal gyrus (Figure 1A and Table 3).

Whole-brain connectivity patterns of the right lateral DLPFC differentiated pregabalin responders from milnacipran responders with 77% accuracy (Figure 1B). Significant average model weights contributing to successful classification included greater connectivity for pregabalin responders versus milnacipran responders to regions including the left precuneus, bilateral superior and inferior parietal lobules, left middle frontal gyrus, right superior frontal gyrus, and the left posterior insular cortex (Table 3). Additionally, significant average model weights where connectivity of the DLPFC was found to be greater in the milnacipran responders as compared to the pregabalin responders included the right anterior cerebellum, right superior frontal gyrus, right middle temporal gyrus, and the right superior temporal gyrus. Many of these connected regions are found to be involved in the frontoparietal, dorsal attention, and sensorimotor networks. The remaining seed regions included in this study did not yield high predictive accuracy. When pretreatment clinical pain ratings were included as an additional feature, the combination model did not improve the predictive power beyond using the whole-brain connectivity maps alone (for left PCC, 77% accuracy; for right lateral DLPFC, 77% accuracy).

In order to enhance classification performance of the aforementioned models, a combinatorial SVM model was produced using connectivity maps from both the left PCC and the right lateral DLPFC. This combinatorial classification model was able to synergistically differentiate responders to pregabalin from responders to milnacipran with 92% accuracy (Figure 1C). Significant average model weights contributing to this result included the combination of those brain regions previously described individually—regions within the default mode network such as the precuneus, PCC, and inferior parietal lobule, the mid cingulate cortex, the posterior insular cortex, the perigenual ACC, and multiple regions within the cerebellum (Figure 1). Complete results are found in Table 3. As with our PCC and DLPFC models alone, the addition of the pretreatment clinical pain ratings did not improve the predictive power of the combined SVM model including the left PCC and right lateral DLPFC, yielding 92% accuracy.

Assessment of confounders and investigation of separation accuracy in SVM classification. To confirm that these significant average model weights of connectivity were specific to responders and not nonresponders for these compounds, the average model weights from these analyses were then applied to the nonresponders from both the pregabalin study (n = 7) and the milnacipran study (n = 8). There were below-chance classification accuracies of 47% for the PCC connectivity maps and 40% for the DLPFC, with the remaining seeds resulting in classification accuracies found to be less than the relevant clinical threshold set for this study (range 13–73%).

We also confirmed that classification weights were specific to pain and not related to changes in anxiety and depression following treatment. In this pregabalin responder versus milnacipran responder analysis, the PCC and DLPFC maps did not yield significant classification for anxiety (left PCC, 15%; right lateral DLPFC, 54%) or depression (left PCC, 54%; right lateral DLPFC, 54%). In an exploratory analysis, responder and nonresponder labels were created for anxiety and depression scores for both the pregabalin and milnacipran groups. The only significant classification in the milnacipran group was for perigenual ACC connectivity, which classified responders versus nonresponders in terms of depression scores, with 73% accuracy (Supplementary Figure 3 and Supplementary Table 2, available on the *Arthritis & Rheumatology* website at http://onlinelibrary.wiley.com/doi/10.1002/art.41781/abstract).

Furthermore, we confirmed that head motion during acquisition of fMRI images did not confound classification performance. For each subject, a composite motion value was created from the average of all time points along the 6 dimensions (3 rotation and 3 translation). This was used to split subjects into high-motion or low-motion groups. The goal was to see if the prediction model obtained from pregabalin responders versus milnacipran responders was able to predict high-motion and low-motion labels. All comparisons yielded below-chance classification, with accuracy ranging from 8% to 31%, demonstrating that the drug classification models obtained from brain images were not confounded by head motion.

We wanted to be sure our classifier was not predicting differences in sequences or MRI hardware between the pregabalin and milnacipran studies despite both studies using the same scan sequences and MRI scanner. When adding baseline placebo scans from both studies, we were unable to differentiate between functional connectivity MRI data from the milnacipran study (n = 15) and the pregabalin study (n = 13) with high accuracy for any seed included in this study (accuracy values ranged from 25% to 64%).

DISCUSSION

FM is a complex condition that is difficult to treat, with pharmacologic interventions providing significant pain relief in only a minority of cases. There has been a recent surge of interest in utilizing candidate pain biomarkers in a predictive, machine-learning framework to improve the management of FM and related chronic pain conditions (18). Here, we utilized machine learning on

Table 3. Significant multivariate SVM prediction of response to pregabalin versus response to milnacipran according to baseline resting-state connectivity between brain regions in patients with FM*

Seed region, regions with significant connectivity weights	Accuracy, %	Size, mm^3	Coordinates		
			x	y	z
Left PCC seed region	77				
Left inferior parietal lobule: BA 40 (−)	–	19,488	−52	−50	44
Left precuneus (−)	–	–	−6	−68	38
Left ventral PCC (−)	–	–	−6	−46	14
Right medial frontal gyrus (−)	–	18,984	6	60	0
Right perigenual ACC (−)	–	–	8	44	−2
Right inferior parietal lobule (−)	–	4,800	46	−50	44
Right medial frontal gyrus/superior frontal gyrus (−)	–	3,296	16	32	42
Right primary motor/primary somatosensory cortex (−)	–	2,744	38	−30	62
Left posterior cerebellum: Crus 1, Crus 2 (−)	–	2,728	−40	−66	−42
Left posterior insular cortex/superior temporal gyrus (−)	–	1,512	−40	−26	14
Right posterior insular cortex (−)	–	744	50	−10	8
Left superior frontal gyrus (−)	–	736	−20	32	46
Right/left superior medial frontal gyrus (+)	–	680	2	60	30
Right superior parietal lobule (+)	–	640	26	−60	60
Right superior temporal gyrus (+)	–	448	56	8	−8
Left superior parietal lobule (+)	–	360	−32	−66	60
Right putamen (−)	–	328	26	16	−2
Right midbrain/pons (−)	–	328	4	−24	−20
Right lateral DLPFC seed region	77				
Right superior parietal lobule (−)	–	36,656	14	−80	54
Right inferior parietal lobule (−)	–	–	46	−46	54
Left precuneus (−)	–	–	−4	−66	44
Left superior parietal lobule (−)	–	–	−16	−70	56
Left inferior parietal lobule (−)	–	–	−40	−62	54
Left primary somatosensory cortex (−)	–	–	−50	−18	58
Left middle frontal gyrus (−)	–	8,184	−24	34	−18
Left inferior frontal gyrus (−)	–	–	−32	30	−12
Right superior frontal gyrus (−)	–	–	34	44	−16
Right pons (−)	–	1,800	20	−14	34
Right parahippocampal gyrus (−)	–	–	22	−4	−28
Left pons (+)	–	1,592	0	−34	−32
Right anterior cerebellum (+)	–	–	10	−48	−28
Left precentral gyrus (−)	–	1,000	−50	−2	26
Right superior frontal gyrus (+)	–	720	16	24	64
Left inferior occipital gyrus (+)	–	544	−44	−78	−6
Right middle temporal gyrus (+)	–	464	52	−6	−22
Right superior temporal gyrus (+)	–	456	42	−50	16
Right posterior cerebellum (+)	–	440	−46	−50	−46
Left posterior insular cortex (−)	–	360	−34	−28	14
Left PCC and right lateral DLPFC seed regions combined	92				
Right superior parietal lobule (−)	–	36,928	34	−50	62
Right primary somatosensory cortex (−)	–	–	58	−18	48
Right inferior parietal lobule: BA 40 (−)	–	–	44	−40	46
Left precuneus (−)	–	–	−8	−64	44
Right precuneus (−)	–	–	6	−62	42
Left inferior parietal lobule: BA 40 (−)	–	–	−40	−50	46
Right perigenual ACC (−)	–	19,408	4	36	−4
Right medial frontal gyrus (−)	–	–	4	58	−6
Left inferior parietal lobule: BA 40 (−)	–	18,800	−48	−50	44
Left precuneus (−)	–	–	−10	−62	42
Left ventral PCC (-)	–	–	−2	−46	20
Left mid cingulate cortex (−)	–	–	−2	−34	46
Left inferior orbital frontal gyrus (−)	–	9,672	−26	30	−10
Right mid orbital frontal gyrus (−)	–	–	18	48	−22
Left precuneus (−)	–	5,072	−6	−42	70
Right mid cingulate (−)	–	–	6	−28	44
Right primary somatosensory cortex (−)	–	2,160	50	−28	62

(Continued)

Table 3. (*Cont'd*)

Seed region, regions with significant connectivity weights	Accuracy, %	Size, mm^3	Coordinates		
			x	y	z
Right anterior cerebellum (+)	–	1,376	10	−48	−24
Right pons (+)	–	–	8	−30	−36
Right supplementary motor area (−)	–	1,176	36	0	58
Left cuneus (+)	–	1,136	−14	−78	8
Left superior frontal gyrus (−)	–	880	−16	28	52
Right supplementary motor area (+)	–	880	14	24	64
Left posterior cerebellum (+)	–	760	−6	−78	−34
Left inferior occipital gyrus (+)	–	696	−48	−82	−4
Left posterior cerebellum (+)	–	496	−42	−52	−50
Right mid temporal gyrus (+)	–	488	50	−4	−20
Left superior parietal lobule (+)	–	472	22	−56	62
Left mid cingulate cortex (−)	–	464	−10	−24	54
Left premotor cortex (+)	–	448	−34	−8	54
Right posterior insular cortex (−)	–	416	44	−10	10
Right posterior cerebellum (+)	–	360	6	−68	−46
Right superior temporal gyrus (+)	–	352	60	10	−8
Right superior frontal gyrus (+)	–	336	14	24	62

* Support vector machine (SVM) accuracy values indicate the frequency with which the model correctly identifies pregabalin responders and milnacipran responders. Group labels were chosen based on median splits (for both drugs, responders had a ≥20 point reduction in pain following treatment), and patients deemed to be responders to each respective drug were entered into this analysis. Results are significant at $P < 0.05$, derived from permutation testing (1,300 iterations), and are reported for clusters >320 mm^3. (+) denotes greater functional connectivity for milnacipran responders compared to pregabalin responders. (−) denotes greater functional connectivity for pregabalin responders compared to milnacipran responders. FM = fibromyalgia; PCC = posterior cingulate cortex; BA 40 = Brodmann area 40; ACC = anterior cingulate cortex; DLPFC = dorsolateral prefrontal cortex.

resting-state fMRI data collected from 2 cohorts of FM patients who underwent longitudinal therapy with pregabalin or milnacipran. The 2 drugs have differential neurochemical properties and mechanisms of action in the central nervous system. Pregabalin is thought to act through inhibition of calcium-dependent release of excitatory neurotransmitters, whereas milnacipran likely works through increasing norepinephrine and serotonin signaling in descending inhibitory pathways (9,10). Therefore, we sought to understand if functional connectivity between brain regions implicated in pain processing and modulation may be a candidate biomarker that predicts differential response to pregabalin and milnacipran in patients with FM.

Machine-learning models showed that baseline patterns of brain connectivity distinguished responders to pregabalin from responders to milnacipran, significantly above the level of chance. To further distinguish that these markers were specific to pain only, we confirmed that improvements in anxiety (left PCC, 15%; right lateral DLPFC, 54%) and depression (left PCC, 54%; right lateral DLPFC, 54%) were not identified by our classifiers. Moreover, motion, scanner, and sequence parameters did not seem to contribute to our results. Finally, our approach did not classify nonresponsiveness to the 2 drugs, suggesting that our markers predict differential analgesic response.

Our results highlight classification differences between milnacipran and pregabalin. We assessed brain connectivity patterns of the PCC, a key node of the default mode network, and found that within–default mode network connectivity patterns were higher in pregabalin responders than in milnacipran responders. Interestingly, our PCC seed region was placed in a dorsal subregion of the PCC which has been found to be associated with pain widespreadness in FM (19), while the resultant connected ventral subregion of the PCC has been shown to be associated with pain catastrophizing in patients with FM (20). This suggests that our classifier identified multiple default mode network regions that influence chronic pain. Further, we explored connectivity of the DLPFC, an antinociceptive node that has shown modifications in connectivity with treatment in previous studies of chronic pain (21). Here we observed that greater connectivity of the DLPFC with subregions of networks including frontoparietal, dorsal attention, and sensorimotor networks differentially predict pregabalin versus milnacipran responders.

Recent machine-learning neuroimaging studies in chronic pain have shown that combining data across different tasks (22) or modalities (23) can bolster classification and prediction accuracy. We combined whole-brain–seed connectivity maps of the PCC and the DLPFC and found increased classification performance (92%) in distinguishing pregabalin versus milnacipran outcomes, which was substantially higher than the individual performance of either seed in isolation (77%). These results underscore the fact that these 2 drugs may act on different brain regions and combining results from different networks can capture unique aspects of pain pathology and bolster classification performance.

In recent years there has been a push toward personalized or precision medicine for numerous medical conditions ranging from cancer to depression (24). Given that most of these conditions are etiologically complex, there are likely multiple pathologies across individuals who share a common diagnosis. The situation is similar for chronic pain. There may be multiple pain-processing pathways wherein plasticity may promote chronic pain that outlasts peripheral nociceptive drive. Therefore, the effectiveness of an analgesic, with a specific set of molecular targets, may be more or less suited to any individual person based on their specific pathology. While the concept of personalized or precision analgesia has been discussed for over 2 decades (25), it still remains largely unrealized for chronic pain.

There are several limitations to this study. The sample size used in this study is small due to the design of our 2 previous studies, and we were unable to include an independent replication cohort. Machine-learning studies typically need larger sample sizes to be robust. Therefore, in future studies, training the model on larger sample sizes with out-of-sample validation is needed to determine if these results are reproducible. Furthermore, to optimize our SVM analyses, we used an unorthodox cutoff to identify our pregabalin and milnacipran responder groups (20% reduction in clinical pain). Studies with larger samples may be able to use a more traditional cutoff point of 30% improvement in pain to identify drug responders. Other machine-learning techniques could have been chosen, but one of our main motivations to use SVM for this study was that it is designed to deal with small sample sizes and high-dimensional data (26). While we were able to achieve high accuracy with leave-one-out cross-validation, we also attempted a k-fold cross-validation analysis where we used a 5-fold cross-validation. This approach yielded the same accuracy values (77% each for the DLPFC and PCC independently, and 92% for the combination of the DLPFC and PCC maps), suggesting that our findings are consistent across multiple methods. Finally, only women were enrolled in this study, and other factors such as age, race, and concurrent medications were not included as part of the SVM.

While our study has limitations, we see this work as a first step toward building robust, generalizable, and predictive markers of pharmacologic response in chronic pain. Machine learning combined with functional connectivity MRI is not yet ready for clinical application. There have been studies that have taken steps to close this gap (27), but it is yet to be confirmed as a viable tool in a clinical setting. To this end, ongoing work will investigate using whole-brain correlation matrices, feature selection techniques, and nonlinear kernels as additional approaches to analgesic prediction.

In summary, our results demonstrate that brain connectivity at baseline, prior to commencing therapy, may be leveraged to differentially predict responders *between* analgesics. The predictive ability may be due to the mechanism of action of these pharmacologic agents on the endogenous pain circuits in the central nervous system. Larger, multisite, and systematic trials with multimodal biomarkers are needed in the future to validate these findings and utilize them in a precision medicine framework.

AUTHOR CONTRIBUTIONS

All authors were involved in drafting the article or revising it critically for important intellectual content, and all authors approved the final version to be published. Dr. Ichesco had full access to all of the data in the study and takes responsibility for the integrity of the data and the accuracy of the data analysis.

Study conception and design. Pauer, Harte, Clauw, Harris.
Acquisition of data. Ichesco, Peltier.
Analysis and interpretation of data. Ichesco, Peltier, Mawla, Harper, Harte, Clauw, Harris.

ROLE OF THE STUDY SPONSORS

Pfizer and Forest Laboratories had no role in the collection, analysis, or interpretation of the data. Nor did Pfizer or Forest Laboratories have any role in writing the manuscript or deciding to submit the manuscript for publication. Pfizer and Forest Laboratories did have a role in study design. Publication of this article was not contingent upon approval by Pfizer or Forest Laboratories.

REFERENCES

1. Clauw DJ. Fibromyalgia: a clinical review. JAMA 2014;311:1547–55.
2. Gracely RH, Petzke F, Wolf JM, Clauw DJ. Functional magnetic resonance imaging evidence of augmented pain processing in fibromyalgia. Arthritis Rheum 2002;46:1333–43.
3. Napadow V, LaCount L, Park K, As-Sanie S, Clauw DJ, Harris RE. Intrinsic brain connectivity in fibromyalgia is associated with chronic pain intensity. Arthritis Rheum 2010;62:2545–55.
4. Kutch JJ, Ichesco E, Hampson JP, Labus JS, Farmer MA, Martucci KT, et al. Brain signature and functional impact of centralized pain: a multidisciplinary approach to the study of chronic pelvic pain (MAPP) network study. Pain 2017;158:1979–91.
5. Derry S, Cording M, Wiffen PJ, Law S, Phillips T, Moore RA. Pregabalin for pain in fibromyalgia in adults. Cochrane Database Syst Rev 2016;9:CD011790.
6. Derry S, Gill D, Phillips T, Moore RA. Milnacipran for neuropathic pain and fibromyalgia in adults. Cochrane Database Syst Rev 2012:CD008244.
7. Arnold LM, Clauw DJ, Wohlreich MM, Wang F, Ahl J, Gaynor PJ, et al. Efficacy of duloxetine in patients with fibromyalgia: pooled analysis of 4 placebo-controlled clinical trials. Prim Care Companion J Clin Psychiatry 2009;11:237–44.
8. Tracey I, Woolf CJ, Andrews NA. Composite pain biomarker signatures for objective assessment and effective treatment. Neuron 2019;101:783–800.
9. Harris RE, Napadow V, Huggins JP, Pauer L, Kim J, Hampson J, et al. Pregabalin rectifies aberrant brain chemistry, connectivity, and functional response in chronic pain patients. Anesthesiology 2013;119:1453–64.
10. Schmidt-Wilcke T, Ichesco E, Hampson JP, Kairys A, Peltier S, Harte S, et al. Resting state connectivity correlates with drug and placebo response in fibromyalgia patients. Neuroimage Clin 2014;6:252–61.
11. Cleeland CS, Ryan KM. Pain assessment: global use of the Brief Pain Inventory [review]. Ann Acad Med Singap 1994;23:129–38.
12. Bjelland I, Dahl AA, Haug TT, Neckelmann D. The validity of the Hospital Anxiety and Depression Scale: an updated literature review. J Psychosom Res 2002;52:69–77.
13. Greicius MD, Krasnow B, Reiss AL, Menon V. Functional connectivity in the resting brain: a network analysis of the default mode hypothesis. Proc Natl Acad Sci U S A 2003;100:253–8.
14. Whitfield-Gabrieli S, Nieto-Castanon A. Conn: a functional connectivity toolbox for correlated and anticorrelated brain networks. Brain Connect 2012;2:125–41.

15. Calhoun VD, Adali T, Pekar JJ. A method for comparing group fMRI data using independent component analysis: application to visual, motor and visuomotor tasks. Magn Reson Imaging 2004;22:1181–91.
16. Hu X, Le TH, Parrish T, Erhard P. Retrospective estimation and correction of physiological fluctuation in functional MRI. Magn Reson Med 1995;34:201–12.
17. Chang CC, Lin CJ. LIVSVM: a library for support vector machines. ACM Trans Intell Syst Technol 2011;2:27.
18. Van der Miesen MM, Lindquist MA, Wager TD. Neuroimaging-based biomarkers for pain: state of the field and current directions [review]. Pain Rep 2019;4:e751.
19. Ellingsen DM, Beissner F, Alsady TM, Lazaridou A, Paschali M, Berry M, et al. A picture is worth a thousand words: linking fibromyalgia pain widespreadness from digital pain drawings with pain catastrophizing and brain cross-network connectivity. Pain 2020;162:1352–63.
20. Lee J, Protsenko E, Lazaridou A, Franceschelli O, Ellingsen DM, Mawla I, et al. Encoding of self-referential pain catastrophizing in the posterior cingulate cortex in fibromyalgia. Arthritis Rheumatol 2018;70:1308–18.
21. Čeko M, Shir Y, Ouellet JA, Ware MA, Stone LS, Seminowicz DA. Partial recovery of abnormal insula and dorsolateral prefrontal connectivity to cognitive networks in chronic low back pain after treatment. Hum Brain Mapp 2015;36:2075–92.
22. López-Solà M, Pujol J, Wager TD, Garcia-Fontanals A, Blanco-Hinojo L, Garcia-Blanco S, et al. Altered functional magnetic resonance imaging responses to nonpainful sensory stimulation in fibromyalgia patients. Arthritis Rheumatol 2014;66:3200–9.
23. Lee J, Mawla I, Kim J, Loggia ML, Ortiz A, Jung C, et al. Machine learning-based prediction of clinical pain using multimodal neuroimaging and autonomic metrics. Pain 2019;160:550–60.
24. National Research Council. Toward precision medicine: building a knowledge network for biomedical research and a new taxonomy of disease. Washington, DC: The National Academic Press; 2011.
25. Woolf CJ, Max MB. Mechanism-based pain diagnosis: issues for analgesic drug development. Anesthesiology 2001;95:241–9.
26. LaConte S, Strother S, Cherkassky V, Anderson J, Hu X. Support vector machines for temporal classification of block design fMRI data. Neuroimage 2005;26:317–29.
27. Wager TD, Atlas LY, Lindquist MA, Roy M, Woo CW, Kross E. An fMRI-based neurologic signature of physical pain. N Engl J Med 2013;368:1388–97.